Separation Science and Technology
Publication details, including instructions for authors and subscription information:
http://www.informaworld.com/smpp/title~content=t713708471

Soil Clean up by *in-situ* Aeration. XI. Cleanup Time Distributions for Statistically Equivalent Variable Permeabilities

Linda A. Roberts[a]; David J. Wilson[a]
[a] DEPARTMENT OF CHEMISTRY, VANDERBILT UNIVERSITY, NASHVILLE, TENNESSEE

To cite this Article Roberts, Linda A. and Wilson, David J.(1993) 'Soil Clean up by *in-situ* Aeration. XI. Cleanup Time Distributions for Statistically Equivalent Variable Permeabilities', Separation Science and Technology, 28: 8, 1539 — 1559
To link to this Article: DOI: 10.1080/01496399308018057
URL: http://dx.doi.org/10.1080/01496399308018057

SEPARATION SCIENCE AND TECHNOLOGY, 28(8), pp. 1539–1559, 1993

Soil Clean Up by *in-situ* Aeration. XI. Cleanup Time Distributions for Statistically Equivalent Variable Permeabilities

LINDA A. ROBERTS and DAVID J. WILSON*
DEPARTMENT OF CHEMISTRY
VANDERBILT UNIVERSITY
NASHVILLE, TENNESSEE 37235

ABSTRACT

The effect of spatial variations in the pneumatic permeability on soil vapor extraction (SVE) cleanup times is explored. Several ways for generating families of permeability functions are discussed, and the characteristics of the resulting functions are examined. The results of eight data sets of 10 runs each are presented. Rather substantial variations in cleanup time are found even for runs using permeability functions drawn from the same family. Rate of cleanup correlates somewhat with average permeability, but this correlation leaves a good deal of variation in cleanup time unaccounted for. It is hoped that this work will give a clearer understanding of the uncertainties intrinsic in the modeling of SVE.

INTRODUCTION

The soil vapor extraction technique (SVE, soil venting, soil vapor stripping, soil vacuum extraction) is now commonly used in the remediation of sites having volatile organic compounds (VOCs) in the vadose zone. The U.S. EPA has published a guide (1) and a quite detailed handbook (2) discussing the technique, Hutzler and his co-workers have published a comprehensive review (3), and this was updated in one of our recent papers on SVE (4).

The nature of the SVE technique is such that assessment of its feasibility and design of a system for use in any particular application are quite site-specific. These depend on the site geology (depth to water table, pneumatic permeability of vadose zone soils, presence of overlying impermeable struc-

*To whom correspondence should be addressed.

tures such as floors or parking lots, heterogeneity of soil, presence of natural or other nonvolatile organics) and on the properties of the contaminants present (vapor pressure, water solubility, partition coefficient on organic carbon, and Henry's constant, all at ambient soil temperature). This has led to a good deal of interest in the mathematical modeling of SVE for feasibility studies, data interpretation, and system design. Johnson, Kemblowski, Colthart, and their associates published a number of papers on this (5–7). Hoag, Marley, Cliff, and their coworkers at Vapex (8–10) were among the first to use mathematical modeling techniques in SVE. Cho carried out a comprehensive study in which modeling work was supported by extensive experimental verification (11). Our group has published a number of articles on the mathematical modeling of SVE under a variety of conditions (Refs. 12, 13, and others in this series).

One of the major uncertainties in determining SVE cleanup times is the pneumatic permeability of the vadose zone soil in the domain to be remediated. The well logs at most SVE sites demonstrate that the medium to be stripped is generally rather heterogeneous in character, and one can expect this heterogeneity to be reflected in a permeability which is highly variable in space. The effects of heterogeneities present as low-permeability lenses and strata were explored earlier and found to be quite substantial (14–16). It was apparent that unfortunate placement of a vapor-stripping well with respect to a low-permeability lens could very easily increase the cleanup time by a factor of 2 or, in unfavorable circumstances, a good deal more.

In the present paper we further explore the effects of variability in the pneumatic permeability function tensor (henceforth simply *the permeability*) on SVE cleanup times. Generally the data set one has to work with in SVE modeling includes a minimal number of permeability measurements to characterize the site. One is very fortunate if sufficient data are provided 1) to locate most of the low-permeability strata and lenses (if these types of heterogeneities are predominant) or 2) to calculate a mean value, a standard deviation, and a correlation length for the permeability if its variations are not associated with clearly defined structures. We examine the second case here, with the objective of determining the extent of the uncertainty in a cleanup time which is calculated from data from which it is possible to estimate the mean, standard deviation, and correlation length of the permeability. First we explore some possible ways for constructing such families of permeability functions, after which we use sets of these permeabilities in a SVE model to calculate the cleanup times. These results then give us some idea of the uncertainty in the cleanup time which is associated with the uncertainty inherent in our probabilistic experimental information about the permeability.

RANDOM PERMEABILITY FUNCTIONS

In this section we examine some methods for constructing permeability functions with random variations. First, we must consider the constraints intrinsic in the nature of the types of permeabilities we wish to consider here. In earlier work we considered permeabilities which are discontinuous at the boundaries between strata (16). Here we shall require that the permeability be a continuous function of the space variables. The permeability must also be nonnegative, and, in order that mean values and standard deviations exist, it must have a finite upper bound in the domain of interest. We here address a two-dimensional model, with one horizontal coordinate and one vertical coordinate. This should allow the exploration of the effects of variable permeabilities and simultaneously keep computational requirements within reasonable bounds.

Let us first consider families of permeability functions of the form

$$K(x,y,\{\phi,\psi\}) = \sum_{m}^{M_x} \sum_{n}^{N_y} A_{mn} \sin(m\pi x/L_x + \phi_{mn}) \times \sin(n\pi y/L_y + \psi_{mn}) + \overline{K} \tag{1}$$

or, more compactly,

$$K(x,y,\{\phi,\psi\}) = f(x,y) + \overline{K} \tag{2}$$

where the family is determined by the set of coefficients A_{mn} and the value of $\overline{K}$, and a particular member of the family is determined by the choice of the set of random phase angles (ϕ_{mn},ψ_{mn}). A set of these phase angles is selected randomly on the interval $(0, 2\pi)$ to specify a particular permeability function in the family. Note that each phase angle, ϕ_{mn} and ψ_{mn}, is selected randomly and independently of all the others. Here L_x and L_y are the dimensions of the domain of interest in the x- and y-directions, and M_x and N_y, the upper limits to the double summation, are determined by the minimum wavelength of variation one wishes to consider, usually determined in modeling computations by the dimensions of the volume elements used in the model.

We would like to explore the statistical properties of these families of permeability functions. This can either be done by carrying out the necessary averaging by first integrating over the space coordinates and then integrating over the phases, or by first integrating over the phases and then integrating (if necessary) over the space coordinates. The second approach is much easier than the first. We let $\langle g \rangle$ be the average of $g(x,y,\{\phi,\psi\})$ over the uniformly distributed random phases $\{\phi,\psi\}$, where g is any function of x, y, and the set $\{\phi,\psi\}$. Averaging a function over a single phase angle involves integrating that function with respect to the phase angle over the interval (0, 2π) and dividing by 2π. Averaging over the entire set of phase angles involves $2M_xN_y$ integrations and division by $(2\pi)^{2M_xN_y}$. Thus, the phase average of K is given by

$$\langle K(x,y)\rangle = \sum_{m}^{M_x} \sum_{n}^{N_y} A_{mn} \langle \sin (m\pi x/L_x + \phi_{mn})\rangle\langle \sin (n\pi y/L_y + \psi_{mn})\rangle + \overline{K} \tag{3}$$

The phase averages of the sine factors are all zero, so the phase average of K is given by

$$\langle K(x,y)\rangle = \langle K\rangle = \overline{K} \tag{4}$$

The phase-averaged mean square deviation of K is given by

$$\langle \sigma_K\rangle^2 = \langle K^2\rangle - \langle K\rangle^2 \tag{5}$$

Now

$$K^2 = \sum_{m}^{M_x} \sum_{n}^{N_y} \sum_{m'}^{M_x} \sum_{n'}^{N_y} A_{mn}A_{m'n'} \sin (m\pi x/L_x + \phi_{mn}) \sin (m'\pi x/L_x + \phi_{m'n'})$$
$$\times \sin (n\pi y/L_y + \psi_{mn}) \sin (n'\pi y/L_y + \psi_{m'n'}) + 2f(x,y)\langle K\rangle + \langle K\rangle^2 \tag{6}$$

From our work above, the phase average of $f(x,y)$ vanishes, so we have

$$\langle K^2\rangle - \langle K\rangle^2 = \sum_{m} \sum_{m'} \sum_{n} \sum_{n'} A_{mn}A_{m'n'}$$
$$\times \langle \sin (m\pi x/L_x + \phi_{mn}) \sin (m'\pi x/L_x + \phi_{m'n'})$$
$$\times \sin (n\pi y/L_y + \psi_{mn}) \sin (n'\pi y/L_y + \psi_{m'n'})\rangle \tag{7}$$

Any terms in Eq. (7) for which m is not equal to m' and/or for which n is not equal to n' average to zero. The remaining terms are all of the form

$$T_{mnmn} = \langle \sin^2 (m\pi x/L_x + \phi_{mn}) \sin^2 (n\pi y/L_y + \psi_{mn})\rangle \tag{8}$$

which yields

$$T_{mnmn} = \langle \sin^2 (m\pi x/L_x + \phi_{mn})\rangle\langle \sin^2 (n\pi y/L_y + \psi_{mn})\rangle \tag{9}$$
$$= (1/2)(1/2) = 1/4 \tag{10}$$

So we have

$$\langle K^2\rangle - \langle K\rangle^2 = (1/4) \sum_{m} \sum_{n} A_{mn}^2 \tag{11}$$

Then

$$\langle \sigma_K \rangle = \tfrac{1}{2}\left[\sum_m \sum_n A_{mn}^2\right]^{1/2} \tag{12}$$

gives us the phase average standard deviation of the permeability. Note that the phase averages $\langle K \rangle$ and $\langle \sigma_K \rangle$ are independent of x and y, so that we need not carry out averages over these variables. The technique of phase averaging is commonly used in classical statistical mechanics.

There is another piece of information about the permeability which is of considerable importance; this is its correlation length. This gives information about the following question: If one measures the permeability to be K_0 at a particular point (x_0,y_0) in the domain, how far from this point can one go [to some new point (x,y)] and still have K_0 be at least a reasonable approximation to $K(x,y)$? Obviously we would generally expect that correlation lengths in the vertical direction will differ from correlation lengths in horizontal directions, and there is a possibility that the correlation length in the horizontal plane will depend upon direction. In the following we shall be concerned with correlation lengths in the x-direction; the extension to other directions is straightforward.

We explore this question by first calculating the autocorrelation function of the permeability in the x-direction, phase averaging, and then determining the value of the least positive root of this phase-averaged autocorrelation function. The procedure is as follows.

The autocorrelation function $C_x(r,y,\{\phi,\psi\})$ is defined as

$$C_x(r,y,\{\phi,\psi\}) = \frac{1}{L_x}\int_0^{L_x} [K(x,y) - \langle K \rangle][K(x + r,y) - \langle K \rangle]dx \tag{13}$$

Use of Eqs. (2) and (4) permits us to write Eq. (13) as

$$C_x(r,y,\{\phi,\psi\}) = \frac{1}{L_x}\int_0^{L_x} f(x,y)f(x + r,y)dx \tag{14}$$

Phase averaging Eq. (14) then yields

$$\langle C_x(r,y) \rangle = \frac{1}{L_x}\int_0^{L_x} \langle f(x,y)f(x + r,y) \rangle dx \tag{15}$$

or, on replacing f by its expression as a double trigonometric series,

$$\begin{aligned} \langle C_x(r,y) \rangle = \frac{1}{L_x}\int_0^{L_x} \sum_m \sum_n \sum_{m'} \sum_{n'} A_{mn}A_{m'n'} \langle &\sin (m\pi x/L_x + \phi_{mn}) \\ &\times \sin (m'\pi x/L_x + \phi_{m'n'} + m'\pi r/L_x) \\ &\times \sin (n\pi y/L_y + \psi_{mn}) \sin (n'\pi y/L_y + \psi_{m'n'}) \rangle \end{aligned} \tag{16}$$

The terms in the sum vanish unless $m = m'$ and $n = n'$ as a result of the phase averaging, so

$$\langle C_x(r,y)\rangle = \frac{1}{L_x}\int_0^{L_x} \sum_m \sum_n A_{mn}^2 \langle \sin(m\pi x/L_x + \phi_{mn}) \times \sin(m\pi x/L_x + \phi_{mn} + m\pi r/L_x)\rangle\langle \sin^2(n\pi y/L_y + \psi mn)\rangle dx \tag{17}$$

The phase average of the sine-squared term gives a factor of ½, as before. The product of sines involving x is handled by means of a trigonometric identity, as follows:

$$\langle \sin(m\pi x/L_x + \phi_{mn}) \sin(m\pi x/L_x + \phi_{mn} + m\pi r/L_x)\rangle = \tfrac{1}{2}\langle \cos(m\pi r/L_x) + \cos(2m\pi x/L_x + 2\phi_{mn} + m\pi r/L_x)\rangle \tag{18}$$

The phase average of the term containing $2\phi_{mn}$ vanishes; the other yields ½ $\cos(m\pi r/L_x)$. Substitution of these results in Eq. (17) and integration with respect to x then gives

$$\langle C_x(r,y)\rangle = \tfrac{1}{4}\sum_m \sum_n A_{mn}^2 \cos(m\pi r/L_x) \tag{19}$$

We see that $C_x(0,y)$ is given by the mean square deviation, which is always positive. We define the phase-averaged correlation length l_c as the least positive root r_1 of Eq. (19).

If we are fortunate, we will have three pieces of experimental information—the mean permeability, its standard deviation, and its correlation length. In our theoretical expressions we have $M_xN_y + 1$ constants—the A_{mn} and $\overline{K}$. Evidently we must make some assumptions about the A_{mn} if we are to progress further; we can evaluate no more than three independent constants from our three pieces of experimental information. Therefore, let us assume that the A_{mn} are of the form

$$A_{mn} = \frac{1}{(m^2 + n^2)^\alpha} \tag{20}$$

where α is a parameter controlling the magnitude of the higher order (shorter wavelength) terms in the Fourier series. A large value of α yields rapidly vanishing higher order terms, resulting in a large correlation length $\langle l_c\rangle$. A small value of α results in coefficients of the higher order terms which are of significant size, resulting in a small correlation length.

The correlation length $\langle l_c\rangle$ can then be used with Eqs. (19) and (20) to calculate the value of α; one substitutes Eq. (20) into Eq. (19), sets the left-hand side of Eq. (19) to zero, replaces r by $\langle l_c\rangle$ on the right-hand side of Eq. (19), and solves the result, Eq. (21), for α numerically.

$$0 = \sum_m \sum_n \frac{\cos (m\pi\langle l_c\rangle / L_x)}{(m^2 + n^2)^{2\alpha}} \tag{21}$$

This is done by a simple search routine which determines for what values of α the right-hand side of Eq. (21) changes sign, and then progressively refines this interval.

The constant A is then obtained from Eqs. (12) and (20) in terms of $\langle\sigma_K\rangle$; the result is

$$A = \frac{2\langle\sigma_K\rangle}{\left[\sum_m \sum_n (m^2 + n^2)^{-2\alpha}\right]^{1/2}} \tag{22}$$

Lastly, we recall from Eq. (4) that

$$\langle K\rangle = \overline{K} \tag{23}$$

Thus we have the three model parameters determined in terms of the correlation length, the root mean square deviation of the permeability, and the mean value of the permeability.

We note that use of excessively large root mean square deviations $\langle\sigma_K\rangle$ can result in negative values of the permeability function at some points, so must be avoided. Practically, this problem does not appear to arise if $\langle\sigma_K\rangle < \frac{1}{3}\langle K\rangle$.

The random phase Fourier series appearing on the right-hand side of Eq. (3) can also be used to generate more complex functions which may be of use in defining randomly varying permeabilities with particular characteristics. Let

$$f(x,y,\{\phi,\psi\}) = \sum_m \sum_n A_{mn} \sin (m\pi x/L_x + \phi_{mn}) \sin (n\pi y/L_y + \psi_{mn}) \tag{24}$$

as before. Then families of functions f can be used to calculate new families of permeability functions by means of such equations as

$$K_1 = \frac{K_0}{1 + [f(x,y)]^2} \tag{25}$$

$$K_2 = \frac{K_0}{1 + |f(x,y)|} \tag{26}$$

$$K_3 = K_0 \exp [- f^2(x,y)] \tag{27}$$

$$K_4 = K_0 \exp [- |f(x,y)|] \tag{28}$$

and so forth.

One pays a price for this increase in flexibility, however, in that the only model parameter which can be readily approximated from the experimental data is K_0, which is an upper bound to the permeability. Correlation lengths, mean permeabilities, and mean square deviations must all be calculated numerically, so that fitting the model parameters A and α by means of the experimental quantities is of necessity a laborious numerical process. Still, there are some advantages. These functions all give permeability values which most certainly lie between zero and K_0, with no possibility of negative values. Their use allows one to obtain different types of distributions of permeability than are possible with the simple Fourier series. Some of these functions may lead to permeabilities which are unrealistic; for instance, K_2 and K_4 show cusp maxima with discontinuous slopes at points where $f(x,y) = 0$. Such cusps are not observed in practice, so these two functions must be discarded. The behaviors of both K_1 and K_3 are reasonable over a range of parameter values, with smoothly varying maxima.

We next examine some sets of plots of K versus x for fixed y, A, and α. We shall also examine the mean values, standard deviations, and mean correlation lengths of some sets of these plots to determine the extent to which the procedure described above permits us to calculate permeability functions with specified mean values, standard deviations, and correlation lengths. One is by no means sure that the use of phase averages, as described above, to specify the model parameters will in fact lead to individual permeability functions having the desired properties. We then turn to an examination of the behaviors of the permeability functions K_1 and K_3, defined above. The objective is to get some feeling for the types of permeabilities which are best represented by these functions.

MODEL RESULTS, PERMEABILITIES

Properties of the Permeability Function $K(x,y)$ Defined by Eqs. (3) and (20)

Sets of 20 permeability functions $K(x,y)$ were generated and their average mean values (averages of 20 mean values), average standard deviations, and average correlation lengths were calculated, along with the standard deviations of each of the quantities being averaged. The default model parameters are given in Table 1. Twenty sets of 20 runs each were made, with values of $\langle l_c \rangle$ ranging from 5 to 14 m, with the results shown in Table 2.

TABLE 1
Default Model Parameters for the Calculations of $K(x,y)$

$\langle K \rangle = 1\ m^2/atm{\cdot}s$
$\langle \sigma_K \rangle = 0.3\ m^2/atm{\cdot}s$
$L_x = 30$ m
$L_y = 20$ m
$M_x = 30$
$N_y = 20$
$y = 10$ m

Regression lines of the three calculated quantities against $\langle l_c \rangle$ were calculated from these data; they are as follows.

$$\overline{K} = (0.991 \pm 0.019) + (0.0007 \pm 0.0024)\langle l_c \rangle, \qquad r^2 = 0.0048 \quad (29)$$

$$\overline{\sigma_K} = (0.346 \pm 0.011) - (0.0084 \pm 0.0013)\langle l_c \rangle, \qquad r^2 = 0.682 \quad (30)$$

$$\overline{l_c} = (1.140 \pm 0.076)\langle l_c \rangle - (3.63 \pm 0.77), \qquad r^2 = 0.913 \quad (31)$$

TABLE 2
Statistical Properties of Calculated Permeability Functions $K(x,y)$, 20 runs per set, 20 sets

$\langle l_c \rangle$ (m)	$\overline{K}$ ($m^2/atm{\cdot}s$)	$\langle \sigma_K \rangle$	$\overline{l_c}$ (m)
5	0.9859 ± 0.0591	0.2966 ± 0.0525	3.64 ± 2.94
5	0.9889 ± 0.0658	0.2904 ± 0.0523	2.55 ± 2.06
6	1.0275 ± 0.0503	0.2973 ± 0.0495	2.58 ± 1.62
6	0.9805 ± 0.0696	0.2942 ± 0.0455	3.86 ± 2.69
7	1.0075 ± 0.0809	0.2763 ± 0.0315	5.65 ± 5.55
7	0.9917 ± 0.0830	0.2846 ± 0.0515	3.53 ± 1.31
8	1.0101 ± 0.0757	0.2757 ± 0.0428	5.32 ± 5.23
8	0.9815 ± 0.0823	0.2672 ± 0.0423	4.14 ± 3.00
9	0.9876 ± 0.1161	0.2879 ± 0.0533	5.33 ± 3.12
9	0.9887 ± 0.1013	0.2829 ± 0.0544	5.10 ± 2.72
10	1.0161 ± 0.1034	0.2702 ± 0.0725	8.58 ± 6.07
10	0.9822 ± 0.0954	0.2938 ± 0.0606	6.60 ± 2.21
11	1.0276 ± 0.0990	0.2688 ± 0.0676	8.36 ± 4.26
11	1.0108 ± 0.1189	0.2808 ± 0.0851	10.22 ± 5.96
12	1.0369 ± 0.1256	0.2366 ± 0.0610	10.63 ± 5.69
12	0.9282 ± 0.1197	0.2222 ± 0.0808	9.35 ± 6.76
13	1.0429 ± 0.1788	0.2461 ± 0.1008	10.59 ± 4.97
13	0.9442 ± 0.1672	0.2515 ± 0.1109	12.36 ± 7.69
14	1.0351 ± 0.1840	0.2158 ± 0.0869	13.70 ± 6.14
14	0.9825 ± 0.2178	0.1922 ± 0.0915	11.89 ± 5.19

Equation (29) indicates little or no dependence of $\overline{K}$ on $\langle l_c \rangle$, as one would expect on the basis of the phase average of K, which is independent of $\langle l_c \rangle$. Equation (30) shows only a rather weak dependence of $\overline{\sigma_K}$ on $\langle l_c \rangle$; $\langle \sigma_K \rangle$ for all these sets of runs was held constant at 0.3 m^2/atm·s, so one would expect that these root mean square variations would have approximately this value, as is seen.

However, the expected dependence of $\bar{l}_c$ on $\langle l_c \rangle$, $\bar{l}_c = \langle l_c \rangle$, is markedly different from Eq. (31). A possible option is to solve Eq. (30) for $\langle l_c \rangle$ in terms of $\bar{l}_c$ and use the desired value of the correlation length to calculate a value for $\langle l_c \rangle$ for use in generating the desired family of permeabilities. One difficulty with this option is suggested by the rather large standard deviations given in Table 2 for l_c; in some sets of runs with fixed $\langle l_c \rangle$ the calculated values of the correlation length varied by as much as a factor of 3, falling both substantially below and substantially above $\langle l_c \rangle$ itself. See Fig. 1 for a plot of average correlation lengths versus $\langle l_c \rangle$; this also illustrates the variability of the results. Thus one has no guarantee that following this procedure will generate a family of permeability functions having correlation lengths which are close to some specified value. A crude but feasible solution is to simply generate permeability functions from the desired parameter set (mean permeability, standard deviation of the permeability, and correlation length), compute correlation lengths for these, and discard those functions which give correlation lengths lying outside of the desired range.

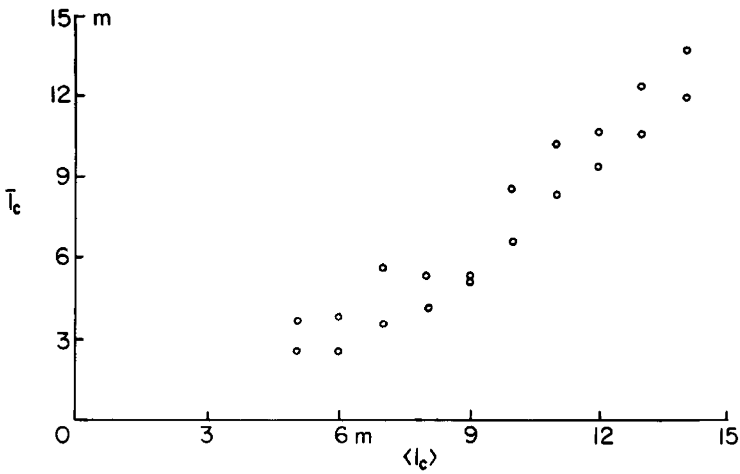

FIG. 1 Plot of mean correlation length $\bar{l}_c$ (20 runs) versus phase average correlation length $\langle l_c \rangle$. Parameters used in $K(x,y)$ as in Table 1.

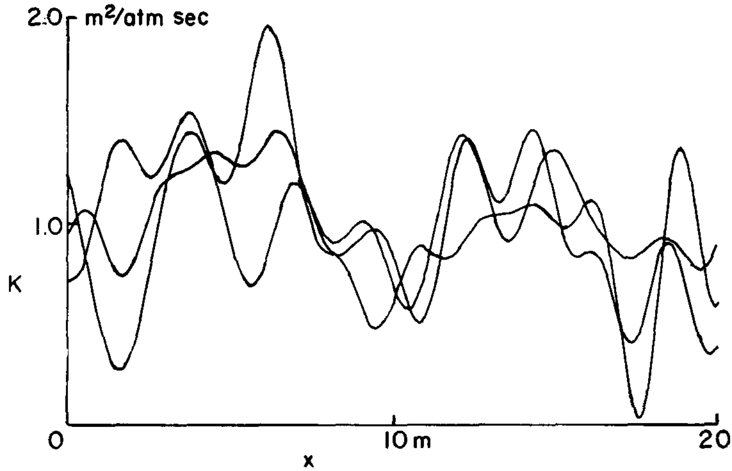

FIG. 2 Representative plots of $K(x,y_0)$ vs x. $\langle K \rangle = 1$ m²/atm·s, $\langle \sigma_K \rangle = 0.3$, $\langle l_c \rangle = 3$ m, $L_x = 20$ m, $L_y = 10$ m, $M_x = 20$, $N_y = 10$, $\alpha = 0.211$, $A = 0.1118$ m²/atm·s, $y_0 = 5$ m.

Plots of some representative permeabilities $K(x,y)$ versus x at constant $y = y_0$ are shown for small and large values of α in Figs. 2 and 3. Parameters not given in the captions are as in Table 1. A plot of the frequency distribution of values of $K(x,y)$ for one of the sets of runs is shown in Fig. 4. This type of distribution, a roughly bell-shaped curve centered approx-

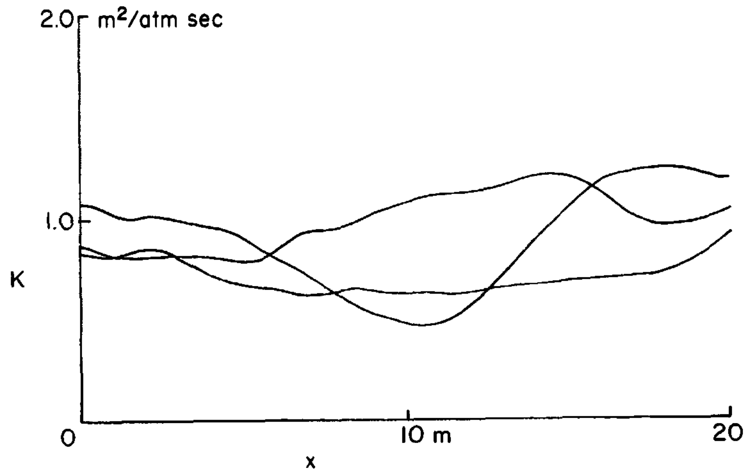

FIG. 3 Representative plots of $K(x,y_0)$ vs x. $\langle K \rangle = 1$ m²/atm·s, $\langle \sigma_K \rangle = 0.3$, $\langle l_c \rangle = 9$ m, $L_x = 20$ m, $L_y = 10$ m, $M_x = 20$, $N_y = 10$, $\alpha = 1.151$, $A = 1.1128$ m²/atm·s, $y_0 = 5$ m.

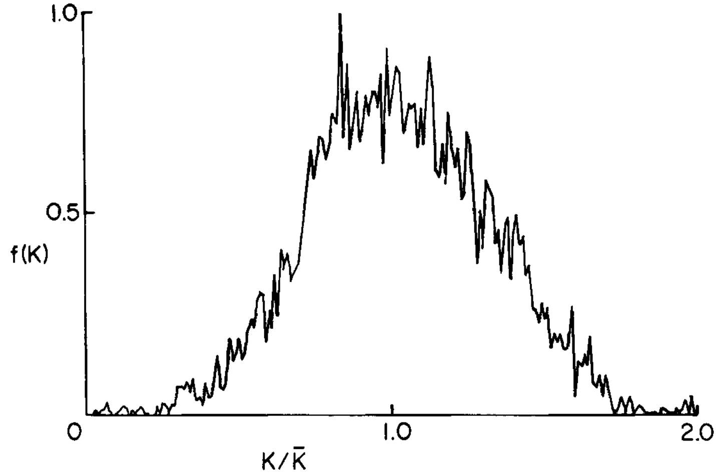

FIG. 4 Frequency distribution of values of $K(x,y_0)$. $\langle K\rangle = 1\ m^2/atm\cdot s$, $\langle\sigma_K\rangle = 0.3$, $\langle l_c\rangle = 6\ m$, $L_x = 30\ m$, $L_y = 20\ m$, $M_x = 30$, $N_y = 20$, $\alpha = 0.296$, $A = 0.1211\ m^2/atm\cdot s$.

imately about the mean value of K, was observed for all of the sets of functions $K(x,y)$ of this type which we examined.

Properties of the Permeability, Functions $K_1(x,y)$ and $K_3(x,y)$ Defined by Eqs. (20), (25), and (27)

The complexities of the functions K_1 and K_3 preclude the sort of detailed analysis which was possible in the previous section. One is limited to selecting values of the parameters K_0, A, and α, calculating a set of representative graphs of permeability versus x or y, and computing numerically such statistical properties of a single permeability function as its mean value and root mean square deviation along a certain direction or over some specified grid of points in space, and its correlation length in the x or y direction for fixed values of y or x. These, however, should be more than sufficient to determine sets of permeability functions which are reasonable representations for the unknown permeability function at a site for which permeability data are few and far between. These, when used in a vapor-stripping model, will then permit us to get some semiquantitative idea of the uncertainty in cleanup time which arises from our lack of detailed knowledge of the permeability throughout the contaminated domain.

The results for the two functions K_1 and K_3 were quite similar, so we focus principally on K_1. Default parameters for the sets of runs are given in Table 3. Twenty data sets of 20 runs each were generated. A statistical

TABLE 3
Default Model Parameters for the Calculations of $K_1(x,y)$

K_{max} = 1 m²/atm·s
L_x = 20 m
L_y = 10 m
M_x = 20
N_y = 10
y = 5 m

summary of the results is given in Table 4, and a plot of $\bar{l}_c$ versus α is shown in Fig. 5. The least squares line fitted to the points plotted in Fig. 5 is

$$\bar{l}_c = (2.088 \pm 0.264)\alpha + (1.948 \pm 0.297) \tag{32}$$

for which r^2 = 0.740. As before, we are faced with the fact that our prescription for generating families of permeability functions yields sets of permeability functions which show a good deal of variation in their correlation lengths. Evidently, if one wishes to specify the correlation length

TABLE 4
Model Parameters and Statistical Results for the Calculations of $K_1(x,y)$, 20 runs per set, 20 sets

α	A	$\bar{K}$ (m²/atm·s)	σ_K	$\bar{l}_c$ (m)
2.00	9.0	0.69	0.17	6.15
1.75	8.0	0.61	0.20	6.45
1.75	7.0	0.61	0.19	5.33
1.50	7.0	0.55	0.24	4.47
1.25	6.0	0.45	0.23	4.14
1.10	5.5	0.52	0.24	3.89
1.00	5.0	0.51	0.25	3.78
0.90	4.5	0.50	0.27	3.97
0.80	4.1	0.46	0.26	3.53
0.75	3.7	0.56	0.27	4.59
0.75	3.8	0.47	0.29	3.51
0.75	3.9	0.41	0.28	3.53
0.75	4.0	0.43	0.27	4.50
0.70	3.0	0.46	0.28	3.23
0.70	4.0	0.39	0.29	3.18
0.65	2.5	0.53	0.29	4.31
0.65	2.6	0.48	0.28	2.74
0.60	2.5	0.49	0.30	3.10
0.55	2.0	0.54	0.30	2.81
0.50	1.5	0.53	0.28	2.26

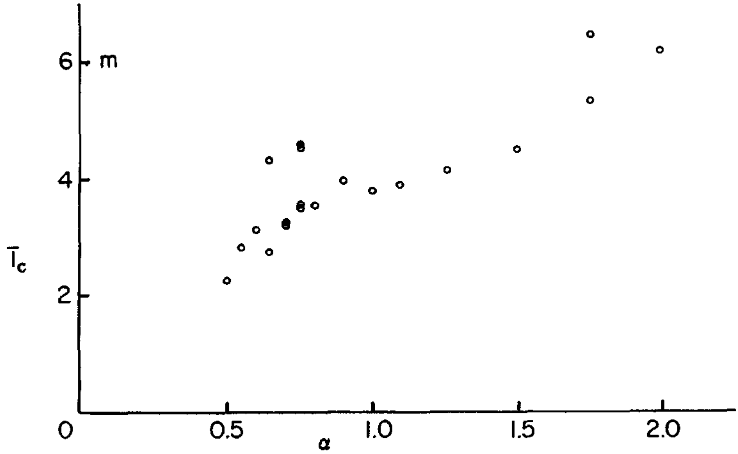

FIG. 5 Plot of mean correlation length $\bar{l}_c$ (20 runs) versus α. Parameters used in $K(x,y)$ as in Table 3.

for a family of functions, one would have to choose a value of α on the basis of Eq. (32) and then generate a large number of permeability functions, discarding those whose correlation lengths were outside the desired interval.

Figures 6 and 7 show some representative plots of permeability functions with small (0.39) and large (1.25) values of α, corresponding to short and

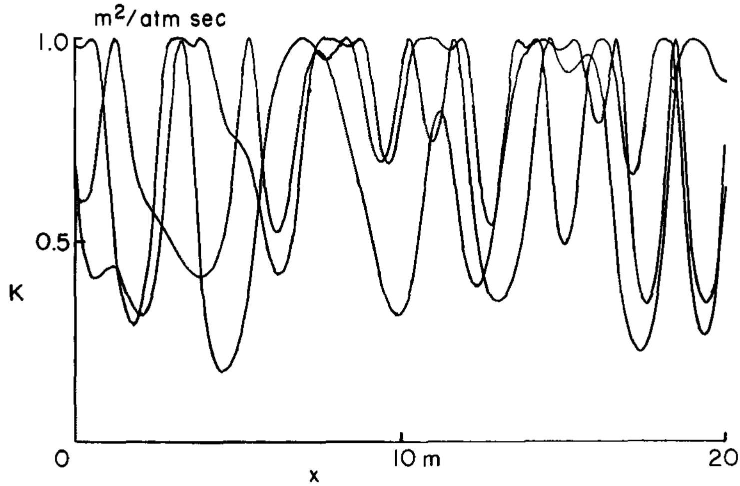

FIG. 6 Representative plots of $K_1(x,y_0)$ vs x. $K_{max} = 1$ m²/atm·s, $\alpha = 0.3946$, $A = 0.4610$, $y_0 = 5$ m, $L_x = 20$ m, $L_y = 10$ m, $M_x = 20$, $N_y = 10$.

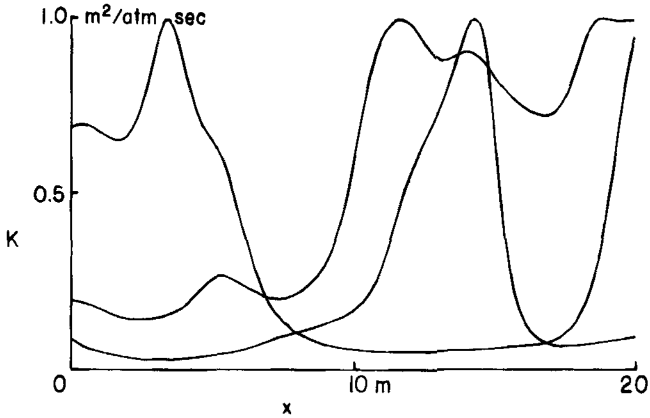

FIG. 7 Representative plots of $K_1(x,y_0)$ vs x. K_{max} = 1 m^2/atm·s, α = 1.25, A = 10, y_0 = 5 m, L_x = 20 m, L_y = 10 m, M_x = 20, N_y = 10.

long correlation lengths. Figure 8 shows the statistical distribution of values of a set of K_1 functions. Here we see some marked differences between $K(x,y)$ and $K_1(x,y)$, as seen by comparing Figs. 4 and 8. The distribution of values of K_1 tends to be bimodal, with a large number of values quite near the upper limit of the permeability, and a broader and lower maximum in the low permeability region. This is the sort of distribution one might

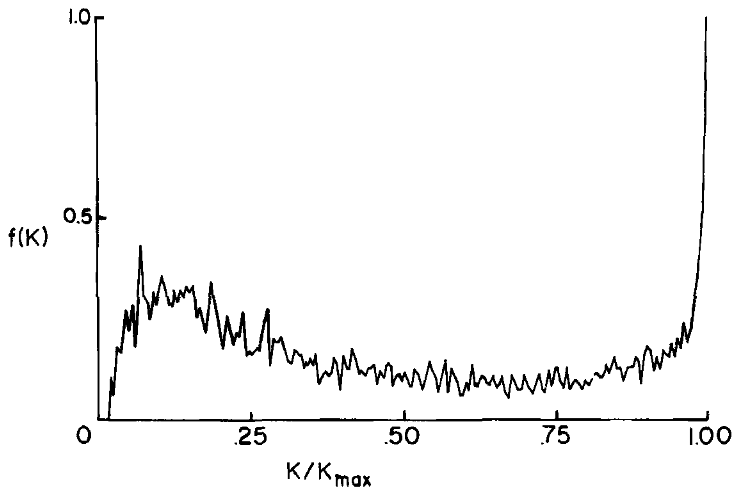

FIG. 8 Frequency distribution of values of $K_1(x,y_0)$. K_{max} = 1 m^2/atm·s, A = 4, α = 0.75, L_x = 20 m, L_y = 10 m, M_x = 20, N_y = 10, y_0 = 5 m.

expect if the site consisted of a fairly high-permeability sand in which there were heterogeneous regions of higher clay content.

The characteristics of the permeability functions $K_3(x,y)$ defined by Eq. (27) were explored; their behavior was sufficiently similar to that of the K_1 functions that detailed investigation was felt unnecessary. Use of K_3 does permit one to generate a relatively large number of quite small permeability values, and might be of interest in situations in which a relatively permeable medium was interspersed with a tight, low-permeability clay.

Soil Vapor Extraction Modeling

A soil vapor extraction model was used with the permeability functions discussed above to simulate SVE remediation in heterogeneous soils. A version of this model has been discussed previously (14); code for the version used here was written by M. M. Megehee (15) for use in another connection. The permeability function is calculated in a subroutine in a program which calculates the soil gas velocity field by a numerical overrelaxation method and writes this information to a file. The file is then read by the program which actually simulates the SVE operation. The model uses a linear isotherm and makes the local equilibrium assumption.

Default SVE model parameter values are indicated in Table 5. Note that the configuration being modeled is that of a buried horizontal slotted pipe, so that Cartesian coordinates (x,y) are used to represent horizontal and vertical distances at right angles to the direction of the pipe. Parameters used to calculate the various families of K_1 functions are given in Table 6; for each of the eight sets of parameters, a set of 10 separate SVE simulations were run, each with its own K_1, defined by the parameter set and its own set of randomly selected phase angles. Cleanup time was defined as the time required to remove 99.9% of the initial mass of contaminant. Cleanup times were determined for all the runs; these are listed in Table 7, along with the average and standard deviations for each set of cleanup times.

TABLE 5
SVE Model Parameters

Width of domain	13 m
Depth of domain	8 m
Number of horizontal divisions	13
Number of vertical divisions	8
Distance of well from left boundary	7 m
Distance of well from top boundary	7 m
Wellhead pressure	0.8959 atm

TABLE 6
Parameters Used in $K_1(x,y)$

File	Maximum permeability, K_{max} (m^2/atm·s)	α	A
8	1.0	0.1	0.8
9	1.0	0.05	0.8
10	1.0	0.2	0.8
11	1.0	0.1	0.2
12	1.0	0.1	0.4
13	0.5	0.1	0.4
14	0.5	0.2	0.8
15	K_H = 1.0, K_V = 0.333 (anisotropic)	0.2	0.8

The maximum and minimum permeability values in the set used in making each run were also determined.

One would expect a correlation between cleanup time and average permeability, and such a relationship is indicated by the data plotted in Fig. 9. Here cleanup time is plotted against the average permeability for each of the eight files. (The average permeability for a file is the average over the 10 runs of the space-averaged permeability.) We see, as expected, a marked tendency for cleanup times to decrease with increasing average permeability, but it is also apparent that this is by no means the only significant factor. This correlation obviously does not take into account any spatial effects. The relationship between the permeability K_{ave} and the average cleanup time for each of the eight sets of runs suggested that we consider a dependence of the form

$$1/t_{99.9} = A\overline{K}_{ave} + B \tag{33}$$

where A and B are constants. A linear least squares fit of the eight points yielded

$$A = 0.0296 \pm 0.0017$$

$$\dot{B} = 0.0017 \pm 0.0011$$

with $r^2 = 0.899$. A linear least squares fit of $1/t_{99.9}$ to $\overline{K}$ was then made for all 80 of the runs; the result was

$$1/t_{99.9} = (0.02560 \pm 0.00067)\overline{K} + (0.00020 \pm 0.00032) \tag{34}$$

with $r^2 = 0.857$.

TABLE 7
Results of SVE Simulations

File	K_{ave} (m^2/atm·s)	σ_K	$t_{99.9}$ (days)	$\bar{t}_{99.9}$
8	0.293	0.089	150, 180, 240, 140, 180, 180, 140, 140, 240, 150	174 + 37
9	0.262	0.084	250, 180, 180, 200, 150, 160, 220, 150, 191.5, 249.5	193 + 35
10	0.223	0.057	98.1, 98.5, 224.9, 765.5, 265.4, 78.8, 183.1, 230.9, 100.1, 357.2	240 + 195
11	0.690	0.064	57.8, 52.9, 52.8, 52.0, 56.4, 55.3, 53.6, 52.9, 58.0, 53.4	54.5 + 2.1
12	0.484	0.093	82.2, 75.2, 75.6, 69.0, 70.8, 71.8, 67.8, 72.2, 82.5, 67.9	73.5 + 5.1
13	0.248	0.024	122.2, 89.8, 104.1, 99.0, 106.5, 147.1, 85.1, 96.6, 100.0, 104.3	106 + 17
14	0.091	0.013	275.3, 160.0, 678.4, 1028.2, 520.1, 1132.0, 1650.0, 889.4, 193.1, 399.2	693 + 457
15	0.226 (K_H)	0.059	369.7, 302.1, 117.0, 143.4, 241.6, 687.0, 825.3, 311.9, 531.7, 156.5	369 + 228

A linear least squares fit of $1/t_{99.9}$ against K_{min} was made for all 80 of the runs. Here K_{min} is the minimum value of the permeability used in the SVE modeling calculations for a particular run. The result is

$$1/t_{99.9} = (0.1040 \pm 0.0084)K_{min} + (0.00476 \pm 0.00039) \qquad (35)$$

with $r^2 = 0.717$. A linear least squares fit of $1/t_{99.9}$ against K_{min} and $\overline{K}$ was also made for all of the runs. This yielded

$$1/t_{99.9} = 0.028275K_{min} + 0.020244\overline{K} + 0.0009388 \qquad (36)$$

with $r^2 = 0.872$.

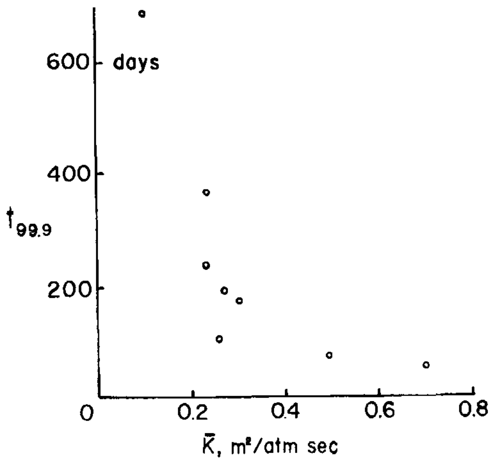

FIG. 9 Plot of average cleanup time (days) vs average permeability for the eight files of SVE simulations using $K_1(x,y)$. See Tables 6 and 7 for parameters and results.

CONCLUSIONS

Fourier series techniques involving the use of randomly selected phase angles have been used to generate families of pneumatic permeability functions having specified characteristics. These permeability functions have been used in a soil vapor extraction model to explore the effect of spatial variations in the permeability on SVE cleanup times.

One of the more interesting of the conclusions which can be drawn from the cleanup time results is that the effects of the heterogeneity introduced into the pneumatic permeability by functions of the type $K_1(x,y)$ within a single set can be quite substantial indeed. The very large standard deviations of the cleanup times for file numbers 8, 9, 10, 14, and 15 give some idea of the uncertainties in cleanup times which can be expected if there is a substantial amount of variation in the permeability. The relatively poor r^2 values for Eqs. (34)–(36) give a clear indication that neither the average permeability nor the minimum permeability is by itself an accurate predictor of cleanup time, although the cleanup time certainly has a tendency to depend upon one or the other of these quantities. This weak result is hardly surprising, since such correlations do not take into account the geometrical relationships between the well and domains of low permeability.

It would be imprudent to regard cleanup times estimated by mathematical modeling as being of high accuracy if well log data indicate that the permeability of the soil medium is highly variable. One must be careful in modeling not to encourage expectations regarding the accuracy of cleanup time estimates which are unrealistically high. The techniques presented here provide a means for making estimates of the uncertainty in the calculated cleanup times which results from heterogeneity in the soil permeability. In some of our sets of runs, cleanup times varied by as much as a factor of 5. These results, incidentally, are consistent with Gomez-Lahoz's findings (14). In that work the heterogeneities were low-permeability lenses of specified location and characteristics (14), and these led to highly variable cleanup times, depending on the location(s) of the lens(es) relative to the well.

Finally, these results provide support for the fundamental rule of SVE, which is that you must be able to move air at a reasonable rate through any soil you propose to clean up. Two practical implications of this are as follows: 1) Do not screen SVE wells in formations of low permeability, which will drastically reduce air flow. 2) Try to design wells in such a way as to maintain a substantial pressure gradient across contaminated domains which may be difficult to remediate. That is, don't screen wells over domains of low permeability and don't attempt to remediate domains of low permeability which are toward the outer edge of the well's effective radius of influence.

REFERENCES

1. J. P. Stumbar and J. Rawe, *Guide for Conducting Treatability Studies under CERCLA: Soil Vapor Extraction Interim Guidance*, U.S. EPA Report EPA/540/2-91/019A, September 1991.
2. T. A. Pedersen and J. T. Curtis, *Soil Vapor Extraction Technology Reference Handbook*, U.S. EPA Report EPA/540/2-91/003, February 1991.
3. N. J. Hutzler, B. E. Murphy, and J. S. Gierke, *Review of Soil Vapor Extraction System Technology*, Presented at the Soil Vapor Extraction Technology Workshop, U.S. EPA Office of Research and Development, Edison, New Jersey, June 28–29, 1989.
4. R. E. Osejo and D. J. Wilson, "Soil Clean Up by *in-situ* Aeration. IX. Diffusion Constants of Volatile Organics and Removal of Underlying Liquid," *Sep. Sci. Technol.*, *26*, 1433 (1991).
5. P. C. Johnson, M. W. Kemblowski, and J. D. Colthart, *Practical Screening Models for Soil Venting Applications*, Presented at the Workshop on Soil Vacuum Extraction, U.S. EPA Robert S. Kerr Environmental Research Laboratory (RSKERL), Ada, Oklahoma, April 27–29, 1989.
6. P. C. Johnson, M. W. Kemblowski, J. D. Colthart, D. L. Byers, and C. C. Stanley, *A Practical Approach to the Design, Operation, and Monitoring of In-Situ Soil Venting Systems*, Presented at the Soil Vapor Extraction Technology Workshop, U.S. EPA Risk Reduction Engineering Laboratory (RREL), Edison, New Jersey, June 28–29, 1989.
7. P. C. Johnson, M. W. Kemblowski, and J. D. Colthart, "Quantitative Analysis for the Cleanup of Hydrocarbon-Contaminated Soils by In Situ Soil Venting," *Ground Water*, *28*, 413 (1990).

8. G. E. Hoag and B. L. Cliff, "The Use of the Soil Venting Technique for the Remediation of Petroleum-Contaminated Soils," in *Soils Contaminated by Petroleum: Environmental and Public Health Effects* (E. J. Calabrese and P. T. Kostechi, Eds.), Wiley, New York, 1985.
9. M. C. Marley, S. D. Richter, B. L. Cliff, and P. E. Nangeroni, *Design of Soil Vapor Extraction Systems—A Scientific Approach*, Presented at the Soil Vapor Extraction Technology Workshop, U.S. EPA RREL, Edison, New Jersey, June 28–29, 1989.
10. M. C. Marley, *Development and Application of a Three-Dimensional Air Flow Model in the Design of a Vapor Extraction System*, Presented at the Symposium on Soil Venting, RSKERL, Ada, Oklahoma, April 29–May 1, 1991.
11. J. S. Cho, *Forced Air Ventilation for Remediation of Unsaturated Soils Contaminated by VOC*, U.S. EPA Report EPA/600/2-91/016, July 1991.
12. D. J. Wilson, A. N. Clarke, and J. H. Clarke, "Soil Clean Up by *in-situ* Aeration. I. Mathematical Modeling," *Sep. Sci. Technol.*, *23*, 991 (1988).
13. S. Kayano and D. J. Wilson, "Soil Clean Up by *in-situ* Aeration. X. Vapor Stripping of Mixtures of Volatile Organics Obeying Raoult's Law," *Ibid.*, *27*, 1525 (1992).
14. C. Gomez-Lahoz, J. M. Rodriguez-Maroto, and D. J. Wilson, "Soil Clean Up by *in-situ* Aeration. VI. Effects of Variable Permeabilities," *Ibid.*, *26*, 133 (1991).
15. M. M. Megehee, Unpublished Work.
16. R. D. Mutch, A. N. Clarke, and D. J. Wilson, "In Situ Vapor Stripping Research Project: A Progress Report," in *Proceedings, 2nd Annual Hazardous Materials Conference/Central*, Rosemont, Illinois, March 14–16, 1989, pp. 1–15.

Received by editor October 5, 1992